

Quantum interference of electrons in a ring: tuning of the geometrical phase

R. Capozza^{1,*}, D. Giuliano^{1,2}, P. Lucignano^{1,3,4}, and A. Tagliacozzo^{1,3}

¹ *Dipartimento di Scienze Fisiche Università degli studi di Napoli "Federico II", Napoli, Italy*

² *Dipartimento di Fisica, Università della Calabria and I.N.F.N.,*

Gruppo collegato di Cosenza, Arcavacata di Rende I-87036, Cosenza, Italy

³ *Coherentia-INFM, Monte S. Angelo - via Cintia, I-80126 Napoli, Italy and*

⁴ *SISSA and INFM Democritos National Simulation Center, Via Beirut 2-4, 34014 Trieste, Italy*

(Dated: March 23, 2022)

We calculate the oscillations of the DC conductance across a mesoscopic ring, simultaneously tuned by applied magnetic and electric fields orthogonal to the ring. The oscillations depend on the Aharonov-Bohm flux and of the spin-orbit coupling. They result from mixing of the dynamical phase, including the Zeeman spin splitting, and of geometric phases. By changing the applied fields, the geometric phase contribution to the conductance oscillations can be tuned from the adiabatic (Berry) to the nonadiabatic (Ahronov-Anandan) regime. To model a realistic device, we also include nonzero backscattering at the connection between ring and contacts, and a random phase for electron wavefunction, accounting for dephasing effects.

PACS numbers: 03.65.Vf, 72.10.-d, 73.23.-b, 71.70.Ej

In mesoscopic quantum devices, the wavefunctions of charged particles may acquire a nonzero phase, when undergoing a closed path in a space threaded by external fields. For instance, electrons traveling in an external magnetic flux ϕ pick up an Aharonov-Bohm (AB) phase [1], which can be read out from DC conductance oscillations in an interference device [2]. Also, spin-orbit interaction (SOI) couples orbital and spin electronic degrees of freedom, thus giving rise to an effective, momentum dependent, field, which adds a geometric (topological) [3, 4] phase to the electron wavefunction [5, 6, 7, 8].

Recently, it has been shown that SOI can be controlled by means of voltage gates in III-V semiconducting mesoscopic structures (Rashba effect) [9, 10, 11]. This has aroused a renewed interest in studying transport in ballistic rings, in the presence of Rashba coupling [12, 13, 14, 15, 16]. Yet, it is still controversial under which conditions the spin dynamics adiabatically follows the orbital motion in a device like this and whether the Berry phase can be detected in the oscillations of the transmission altogether [17]. Also, it is, up to now, still unclear, what are the possible consequences of dephasing due to small fluctuations of the length of the arms, or scattering at the connections between the device and the leads.

In this paper, we report extensive results concerning ballistic quantum transport across a $1d$ ring, in the presence of both an orthogonal magnetic field and of SOI. We compute the DC conductance by means of the Landauer formula [18] $G = e^2/\hbar \sum_{\sigma\sigma'} |A(\sigma;\sigma'|E)|^2$, where $A(\sigma;\sigma'|E)$ is the probability amplitude for an electron entering the ring with energy E and spin polarization σ' to exit with spin polarization σ . We employ a real-time path integral approach [19], and we use the saddle point approximation for the orbital motion (which singles out an optimum constant velocity for the electron, $\dot{\varphi}$). At each contact, the transmission is weighted with an

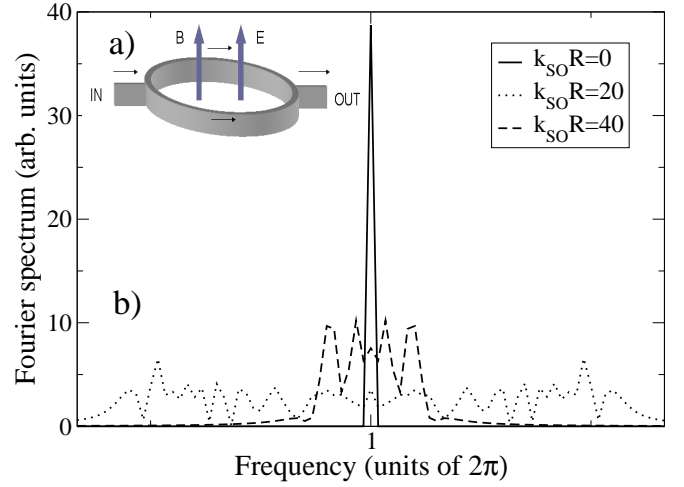


FIG. 1: (color on line) a) Sketch of the device studied, b) Fourier transform of the conductance vs of Fig.(3 [right panel]) for $k_{SO}R = 0, 20, 40$. The variable conjugate to the magnetic flux ϕ/ϕ_0 is in units of 2π

amplitude $\bar{t} e^{iz}$, and the reflection takes place with amplitude $\bar{r} e^{iz}$, where z is a stochastic variable with flat distribution in $[-\zeta, \zeta]$, which encodes dephasing effects. Eventually, we average N times over different dephasing realizations. The winding in the ring before escaping provides the electron propagator with an extra phase, which includes the combined effect of “geometrical” and “dynamical” phases, arising from AB, SOI and Zeeman spin splitting (ZSS) (proportional to the cyclotron frequency ω_c). Our approach applies to any regime, either adiabatic, or nonadiabatic, as the spin propagator is evaluated exactly. In the limiting regimes, in which ZSS is either much larger, or much less, than SOI, the dynamical and the geometrical phases can be easily identified. The intriguing regime is the non adiabatic one, when ZSS

and SOI are of comparable strength.

In Fig.(1 b), we plot the Fourier transform of the interference contribution to the DC conductance for three increasing values of SOI (Fig.3[right panel]), with very little back reflection at the connections between ring and leads, and no dephasing ($\zeta = 0$). In the absence of SOI (solid line), we see only the peak corresponding to AB oscillations. At increasing SOI strength (dotted line), more structures appear, which eventually evolve into a four-peak structure for a larger value of SOI (dashed line). The four-peak feature confirms the interpretation by Yau *et al.* [17] and supports the conclusion that the Berry phase can be detected experimentally in similar devices. We consider the dynamics of a spinful single electron injected at the Fermi energy in a ring with equal arms [20], as sketched in Fig.(1 a). In calculating the transmission in an orthogonal electric and magnetic field, we neglect the actual finite transverse dimension of the arms of the ring, as this would alter the result only quantitatively [21]. Our model Hamiltonian is given by:

$$H = \frac{\hbar^2}{2mR^2} \left(\hat{l} + \frac{\phi}{\phi_0} \right)^2 + \frac{1}{2} \hbar \omega_c \sigma_z + \frac{\alpha}{\hbar} \left(\hat{z} \times \left(\vec{p} + \frac{e}{c} \vec{A} \right) \right) \cdot \vec{\sigma}, \quad (1)$$

where $\hbar \hat{l} = i\hbar \partial_\varphi$ is the angular momentum operator, φ is the orbital coordinate along the ring, and $\vec{\sigma}$ are Pauli matrices; α is a coupling constant, including the effect of the electric field (in units of $eV/\text{\AA}$), $k_{\text{SO}} R = 4\alpha\tau_0/(\hbar R)$, where $\tau_0 = mR^2/2\hbar$ is the time scale of orbital fluctuations (note that $\omega_c = \tau_0^{(-1)} \phi/\phi_0$). Since we are interested in the transmission amplitude in time t_f , $A(\sigma_f, t_f; \sigma_0, 0)$, we sum over paths within homotopy classes, corresponding to the electron winding $n + 1/2$ times in the ring ($n + 1/2$ is positive or negative, depending on whether the electron path winds clockwise, or counterclockwise) [22]. We assume ballistic quantum propagation at energy E_0 (referred to the Fermi energy of the contacts), which requires integrating over all final times $t_f > 0$. Accordingly, the transmission amplitude for an electron entering the ring at $\varphi(0)$ with spin polarization σ_0 and exiting at $\varphi(0) + \pi$, with spin polarization σ_f , for a given realization of the random phases is given by:

$$A(\sigma_f; \sigma_0 | E_0) = |\bar{t}|^2 \sum_{n=-\infty}^{\infty} \int_0^\infty dt_f |\bar{r}|^{2(|n|-1)} e^{i \sum_j^{2|n|} z_j} e^{i \frac{E_0 t_f}{\hbar}} \int_{\varphi(0)}^{\varphi(0) + \pi(2n-1)} \mathcal{D}[\varphi] \langle \sigma_f, t_f | e^{i \int_{t_0}^{t_f} dt \mathcal{L}[\varphi, \dot{\varphi}, t]} | \sigma_0, 0 \rangle. \quad (2)$$

The n^{th} partial amplitude in Eq.(2) corresponds to summing over paths $\varphi(t)$ satisfying the boundary conditions $\varphi(t_f) - \varphi(0) = \pi(2n - 1)$. We take the transparency at the contacts to be such that backscattered trajectories which retrace back part of the path can be neglected. This suppresses weak localization corrections[23] and Altshuler-Aronov-Spivak oscillations[24]. The Lagrangian in Eq.(2) is given by:

$$\mathcal{L}[\varphi(t), \dot{\varphi}(t), \vec{\sigma}] = \frac{m}{2} R^2 \dot{\varphi}^2(t) - \frac{\phi}{\phi_0} \hbar \dot{\varphi}(t) + \frac{\alpha^2 m}{2\hbar^2} + \frac{\hbar^2}{8mR^2} - \left[\frac{1}{2} \hbar \omega_c \sigma_z + \frac{\alpha R m \dot{\varphi}(t)}{\hbar} \left(e^{-i\varphi(t)} \sigma_+ + e^{i\varphi(t)} \sigma_- \right) \right]. \quad (3)$$

We now perform the saddle point approximation on the orbital motion. Since in Eq.(2) the spin is still a quantum operator, we derive the equation of motion for φ within the coherent state representation for spin variables (Haldane's mapping) [25].

$$\frac{d}{dt} \frac{\partial \mathcal{L}}{\partial \dot{\varphi}(t)} - \frac{\partial \mathcal{L}}{\partial \varphi} = 0 \Rightarrow mR^2 \ddot{\varphi}(t) = 0 \quad (4)$$

Thus, the dynamics of the orbital coordinate φ decouples from the spin dynamics, within saddle point approxi-

mation. The solution of Eq.(4) satisfying the appropriate boundary conditions and parametrized by the integer n is

$$\varphi_n(t) = \varphi(0) + \text{sign}(n) \pi (2|n| - 1) \left(\frac{t}{t_f} \right) \quad (5)$$

The ultimate formula for the transmission amplitude across the ring is given by [26]

$$A(\sigma_f; \sigma_0 | E_0) = \sqrt{\frac{m}{2\tilde{E}_0}} |\tilde{t}|^2 \sum_{n \neq 0, n=-\infty}^{\infty} |\tilde{r}|^{2(|n|-1)} e^{\sum_j^{2|n|} z_j} e^{i \frac{m R^2}{2\hbar t_n} (\pi(2|n|-1))^2} e^{-i \frac{\phi}{\phi_0} (\pi(2|n|-1)) \text{sign}(n)} e^{i E_0 t_n / \hbar} \times \quad (6)$$

$$\times e^{i[1+(k_{\text{SO}} R)^2] t_n / 16\tau_0} \langle \sigma_f | \hat{U}_{cl}(t_n, 0) | \sigma_0 \rangle,$$

with $\tilde{E}_0 = E_0 + \hbar [1 + (k_{\text{SO}} R)^2] / 16\tau_0$. In Eq.(6), the spin dynamics is governed by the effective Hamiltonian $\hat{H}_{\text{spin}}(t) = \vec{b}(t) \cdot \vec{\sigma}$. $H_{\text{spin}}(t)$ is parametrized by the angular velocity of the electron rounding $n + 1/2$ times in the ring, $\dot{\varphi}_n$, which is a constant, according to Eq.(5). $H_{\text{spin}}(t)$ is the Hamiltonian of a quantum spin, moving in an effective time dependent external magnetic field $\vec{b}(t) = (b_z, b_-, b_+) = (\frac{\hbar\omega_c}{2}, k_{\text{SO}} R \hbar \dot{\varphi}_n e^{i\varphi_n(t)}/2, k_{\text{SO}} R \hbar \dot{\varphi}_n e^{-i\varphi_n(t)}/2)$. Eq.(6) contains the matrix elements of the spin evolution operator $U_{cl}(t_f, 0) = \hat{T} \exp[-i \int_0^{t_f} H_{\text{spin}}(t) dt]$, (\hat{T} is the usual time-ordering operator), between states with given spin polarization. Such a matrix element adds a geometrical phase to the total amplitude. This phase reduces to the usual Berry phase in the adiabatic limit [3].

To obtain Eq.(6) from Eq.(2) we have used the steepest descent approximation. Within the n^{th} topological sector, we find that the phase of the integrand is stationary at the time $t_n = \pi[(2|n| - 1)\tau_0] \sqrt{\hbar\tau_0/\tilde{E}_0}$. Thus, we evaluate the contribution of each term to the sum of Eq.(2) at $t = t_n$. Inserting Eq.(6) in the Landauer formula allows us to compute the linear conductance across the ring.

In the right panel of Fig.(2), we plot the DC conductance *vs.* $k_{\text{SO}} R$ at $\phi/\phi_0 = 0$ for different values of \bar{r} (different plots within a single box), and at increasing phase randomness (boxes from top to bottom with $\zeta = 0, \pi/3, \pi, 2\pi$), averaged over $N = 1000$ realizations. In the left panel, we plot the DC conductance *vs.* ϕ/ϕ_0 , for the same values of \bar{r} and ζ , at $k_{\text{SO}} R = 0$. In the right panel, we see that in the case of ideal coupling, $\bar{r} = 0$, the quasiperiodic oscillation of the conductance reproduces the localization conditions at the expected values of $k_{\text{SO}} R$ [14, 15, 16]. For $\bar{r} > 0$, interference involving winding numbers $|n + 1/2| > 1$ gives rise to more complicated patterns: the average and the peak value of the conductance decrease, when the transparency of the barriers is lowered. The transmission is progressively reduced, when \bar{r} increases. Contributions from higher harmonics, due to multiple reflections, only appear in the AB oscillations, with maximum amplitude when ϕ/ϕ_0 is close to an integer, that is, when the constructive interference condition is fulfilled.

We see that in both panels in Fig.(2) the amplitude of the oscillations due to quantum interference are overall reduced by the same size, because of increasing ζ . Even-

tually they are washed out for $\zeta = 2\pi$.

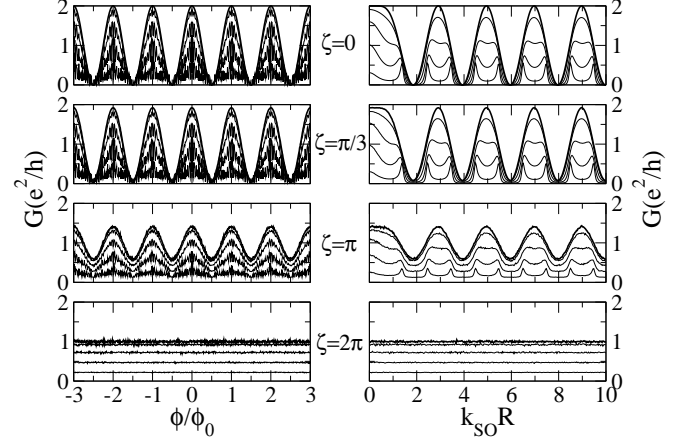


FIG. 2: [Left panel] Conductance *vs.* ϕ/ϕ_0 at $k_{\text{SO}} R = 0$, for $\bar{r} = 0, 0.2, 0.4, 0.6, 0.8$ (different curves from top to bottom in each box) and at increasing dephasing (parametrized by ζ). [Right panel] Conductance *vs.* $k_{\text{SO}} R$ at $\phi/\phi_0 = 0$, for the same values of \bar{r} and ζ .

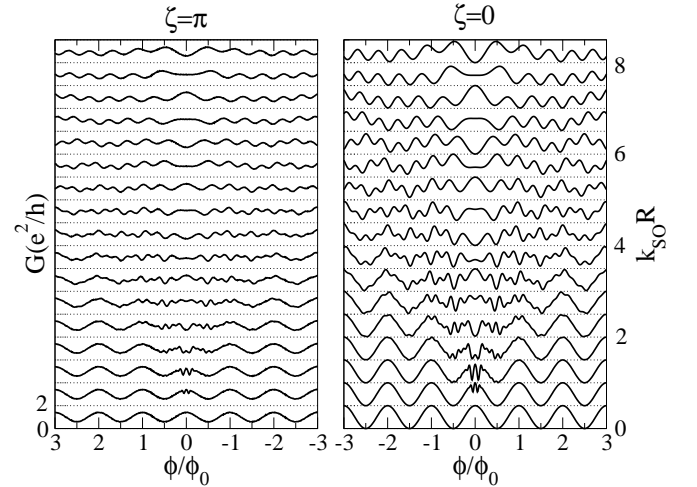


FIG. 3: [Right panel] Conductance *vs.* ϕ/ϕ_0 for increasing values of SOI at $\zeta = 0$ and $\bar{r} = 0.05$. [Left panel] The same plot as at the right panel, but for $\zeta = \pi$.

In Fig.(3), we show the combined effect of B and SOI, on the conductance as a function of ϕ/ϕ_0 at $E_0 = 0$ and $\bar{r} = 0.05$, at increasing values of $k_{\text{SO}} R$ (from bottom to top) for $\zeta = 0$ [right panel], and $\zeta = \pi$ [left panel]. From the right panel, we see that the zero-flux value of the

conductance oscillates with increasing $k_{\text{SO}}R$. Maxima and minima are reduced by the dephasing, as it appears from the left panel, since both constructive, as well as disruptive interference, are suppressed. The results at the right panel are in excellent qualitative agreement with recent experiments [13]. Therefore, we infer that, in real samples the coupling between the contacts and the leads is approximately ideal ($\bar{r} \sim 0$) and the transport is quasi-ballistic.

The geometrical phase should be detectable as a modulation of the interference term in the total DC conductance across the ring, on top of the fundamental modulation due to AB-effect. Fig.(1 b) shows the Fourier transform of the patterns at the right panel of Fig.(3) for $k_{\text{SO}}R = 0, 20, 40$. To get an insight concerning the appearance of the four-peak feature at $k_{\text{SO}}R = 40$, we may resort to the adiabatic approximation for the conductance ($k_{\text{SO}}R\dot{\phi} \ll \omega_c$), obtaining:

$$\sum_{\sigma\sigma'} |A(\sigma; \sigma')|^2 \approx 2 - 2 \sum_{\pm} \left\{ \cos^2 \theta \cos \left[2\pi \frac{\phi}{\phi_0} \pm \pi \cos \theta \right] + \sin^2 \theta \cos \left[\pi \frac{\phi}{\phi_0} \pm \frac{\pi \omega_c}{\dot{\phi}} \right] \right\}, \quad (7)$$

where $\cos \theta = \left[1 + (k_{\text{SO}}R\dot{\phi}/\omega_c)^2 \right]^{-1/2}$.

In the absence of SOI ($\theta = 0$), the former term reduces to the usual AB-oscillating term, while the latter one simply disappears. When SOI is $\neq 0$, but still much smaller than ZSS, θ weakly depends on ϕ , so that two small satellites appear at each side of the AB peak. For $k_{\text{SO}}R = 40$, the Berry phase becomes proportional to ϕ . Hence, the central AB peak splits into two, as seen in Fig.(1 b). Also, since $\cos^2(\theta)$ decreases, while $\sin^2(\theta)$ increases, the amplitude of the outer peaks (associated to ZSS) increases, while the amplitude of the inner peaks (associated to Berry phase) decreases. Therefore, we infer that the splitting of the AB peak into two is, in fact, an evidence for the existence of a topological phase [17, 27].

To conclude, we have employed a path integral real time approach to compute the DC conductance of a ballistic mesoscopic ring in both electrical and magnetic fields. Our approach goes beyond other recent semiclassical calculations by allowing for nonideal couplings between ring and leads (with nonzero reflection \bar{r}) and for dephasing effects. The results satisfactorily compare with experiments.

By varying the external fields we can explore both the adiabatic and nonadiabatic regime: the latter appears as irregular wiggles in the middle of Fig.(3) [right panel]. For large Rashba couplings and a weak magnetic field, spin flip phenomena take place, due to the off-diagonal component of the spin evolution matrix. We stress that $k_{\text{SO}}R = 30 - 40$ corresponds to a SOI coupling $\alpha \sim 200 \text{ meV}\text{\AA}$, in rings with $R \sim 1\mu\text{m}$, what can

be presently achieved experimentally. In this regime such devices can work as spin filters.

We acknowledge valuable discussions with D. Bercioux, G. Campagnano and R. Haug.

* Present address: INFN-S3 e Dipartimento di Fisica, Università di Modena e Reggio Emilia, via Campi 213/A, 41100 Modena, Italy.

-
- [1] Y. Aharonov, D. Bohm, Phys. Rev. **115** 485 (1959).
 - [2] S. Washburn and R. A. Webb, Rep. Prog. Phys. **55**, 1311 (1992).
 - [3] M. V. Berry, Proc. R. Soc. London, A **392**, 45 (1984).
 - [4] Y. Aharonov, J. Anandan, Phys. Rev. Lett. **58**, 1593 (1987).
 - [5] Y. Meir, Y. Gefen, and O. Entin-Wohlman, Phys. Rev. Lett. **63**, 798 (1989).
 - [6] D. Loss, P. Goldbart and A. V. Balatsky, Phys. Rev. Lett. **65**, 1655 (1990); H. A. Engel and D. Loss, cond-mat/0002396v2.
 - [7] D. Bercioux, M. Governale, V. Cataudella, and V. M. Ramaglia Phys. Rev. Lett. **93**, 056802 (2004).
 - [8] A. G. Aronov and Y. L. Lyanda-Geller, Phys. Rev. Lett. **70**, 343 (1993).
 - [9] F. E. Meijer, A. F. Morpurgo, T. M. Klapwijk, T. Koga and J. Nitta, cond-mat/0406106.
 - [10] J. B. Miller, D. M. Zumbühl, C. M. Marcus, Y. B. Lyanda-Geller, D. Goldhaber-Gordon, K. Campman and A. C. Gossard, Phys. Rev. Lett. **90** 076807 (2003).
 - [11] P. Lucignano, B. Jouault and A. Tagliacozzo, Phys. Rev. B **69**, 045314 (2004); P. Lucignano, B. Jouault, A. Tagliacozzo and B. L. Altshuler, Phys. Rev. B **71**, 121310(R) (2005).
 - [12] A. F. Morpurgo, J. P. Heida, T. M. Klapwijk, B. J. van Wees and G. Borghs, Phys. Rev. Lett. **80**, 1050 (1998).
 - [13] J. Nitta, T. Koga, F. E. Meijer, Physica E **18**, 143 (2003); F. E. Meijer, J. Nitta, T. Koga, A. F. Morpurgo, T. M. Klapwijk, Physica E **22**, 402, (2004); M. J. Yang, C. H. Yang, K. A. Cheng and Y. B. Lyanda-Geller, cond-mat/0208260.
 - [14] D. Frustaglia, K. Richter, Phys. Rev. B **69** 235310 (2004).
 - [15] B. Molnár, F. M. Peeters and P. Vasilopoulos, Phys. Rev. B **69**, 155335 (2004);
 - [16] S. Souma and B. K. Nikolić, Phys. Rev. B **70**, 195346 (2004).
 - [17] J. B. Yau, E. P. de Poortere, and M. Shayegan, Phys. Rev. Lett. **88**, 146801 (2002), **90** 119702 (2003), **90** 119704 (2003); A. G. Mal'shukov and K. A. Chao, Phys. Rev. Lett. **90** 119701 (2003); A. G. Wagh, and V. C. Rakhecha, Phys. Rev. Lett. **90** 119703 (2003).
 - [18] R. Landauer, IBM J. Res. Dev. **1** 223 (1957); M. Buttiker, IBM J. Res. Dev. **32** 317 (1988).
 - [19] R. P. Feynmann, *Quantum Mechanics and Path Integral*, Mc Graw-Hill, New York 1965.
 - [20] U. Aeberhard, K. Wakabayashi and M. Sigrist, cond-mat 0411620v1 (2004).
 - [21] A. V. Moroz and C. H. W. Barnes, Phys. Rev. B **60**, 14272 (1999).
 - [22] G. Morandi and E. Menossi, Eur. J. Phys. **5** 49 (1984).
 - [23] By scattering at the contacts, we assume that non ballistic trajectories which contribute to winding number

n but reflect back by retracing some of the path can be neglected. This applies if we are not in the extreme mesoscopic limit (i.e. ring diameter much smaller than the phase coherence length), that is both conditions, $|n| \gg 1$ and $|n|(1 - |r|^2) \sim 1$ are not simultaneously satisfied. Indeed, by our choice of the parameters, contributions for large $|n|$ are always very small.

[24] B.L. Altshuler, A.G. Aronov, B.Z. Spivak, JETP Lett.

33 (1981) 94.

[25] F. D. M. Haldane Phys. Rev. Lett. **50**, 1153 (1983).

[26] Strictly speaking the transmission amplitude of Eq.(6) should exclude the prefactor, which is the same as for the free particle evolution.

[27] A. G. Wagh and V. C. Rackhecha, Phys. Rev. A **48**, 1729(R) (1993).